ELSEVIER

Journal of Contaminant Hydrology 17 (1994) 91–109

JOURNAL OF
Contaminant
Hydrology

Estimating solute transport in undisturbed soil columns using time–domain reflectometry

D. Mallants, M. Vanclooster, M. Meddahi, J. Feyen

Institute for Land and Water Management, Faculty of Agricultural Sciences, Katholieke Universiteit Leuven, B-3000, Leuven, Belgium

Received 29 July 1993; revision accepted 27 June 1994

Abstract

Time–domain reflectometry (TDR) was used to monitor solute breakthrough curves (BTC's) in 30 saturated undisturbed soil columns collected along a 35-m-long transect in the field. The BTC's were obtained by relating the bulk soil electrical conductivity, EC_a, to the relative concentration of a KCl solute pulse applied to the soil surface. Values of EC_a were estimated by measuring the soil's impedance to an electromagnetic wave generated by a cable tester. Parallel two-rod TDR probes inserted horizontally at a depth of 10 cm were used to monitor the soil's impedance during transport of the KCl solute pulse. Calculated experimental time moments indicated that the BTC data were very variable in time and space. This variability was attributed in part to the relatively small volume of soil sampled with the TDR probes, and in part to the natural heterogeneity of the sandy loam soil. The observed BTC's were classified into three groups. One group showed bell-shaped curves consistent with the classical convection–dispersion equation (CDE). A second group was characterized by early breakthrough and long tailing. The BTC's in this group could be described by a mobile–immobile transport model (MIM). A third group of BTC's showed irregular shapes with several peaks. Time moments were used to compare the estimated (from the moments), fitted (CDE and MIM) and independently measured pore-water velocities. The disparities between the observed and fitted velocities suggest that for structured soil several TDR probes may be necessary in order to obtain reasonable estimates of column-scale solute transport behaviour.

1. Introduction

As an ever expanding population puts more and more pressure on the Earth's natural resources, research of environmental problems undoubtedly will remain a high priority issue for many years to come. Of special importance is continued

SSDI 0169-7722(94)00029-H

fundamental and applied research on the subsurface transport of dissolved chemicals migrating from industrial and municipal waste disposal sites, leaky landfills, and of pesticides and fertilizers used in agriculture. Although many early studies of solute transport concentrated on transport processes in laboratory soil columns (Biggar and Nielsen, 1962; van Genuchten and Wierenga, 1977; Tyler and Thomas, 1981; Schulin et al., 1987; Seyfried and Rao, 1987), recently several authors have emphasized the importance of monitoring and predicting solute transport at the field scale (Jury et al., 1982; Butters et al., 1989; Ellsworth et al., 1991; Van Wesenbeeck and Kachanoski, 1991).

Solute concentration distribution in field studies are generally collected using suction sampler techniques. A major drawback of this method is the disturbance of the flow-path of the dissolved tracer when a relatively high suction is applied to the soil matrix (van der Ploeg and Beese, 1977). Other disadvantages are the limited range of moisture contents between saturation and field capacity to which the technique can be applied, and the small sampling volume which increases the variability of the measurements (Hansen and Harris, 1975; Broadbent, 1981). For similar reasons, Alberts et al. (1977) reported significant differences between soil nitrate concentrations determined by either soil coring or solution extraction. van Genuchten and Wierenga (1977) raised the point that soil solution collected using porous cups likely represents mainly mobile water, while solutes within immobile water zones may go undetected. Another popular method for soil sampling is soil coring. Although much more involved and destructive, soil coring is probably the most accurate and reliable in terms of giving estimates of the total resident concentrations. As opposed to suction cup sampling, time-domain reflectometry (TDR) techniques such as those discussed in this paper permit one to collect in situ solute distributions for nonreactive solutes in a nearly undisturbed manner. TDR can also give estimates of the total bulk soil electrical conductivity, as well as the total resident solute concentration if appropriate calibrations have been carried out. TDR applications for determining soil water content are well known for more than ten years (Topp et al., 1982; Topp and Davis, 1985). Recently, TDR is also increasingly being used to monitor solute transport, both in the field as well as in the laboratory (Elrick et al., 1992; Kachanoski et al., 1992; Vanclooster et al., 1993).

In order to study the effects of measurement scale and variability in flow and transport parameters on predicted field-scale solute transport, we collected thirty 20-cm-long and thirty 1-m-long undisturbed columns from a transect in a field near Leuven, Belgium. In this paper we investigate the appropriateness of horizontally installed TDR probes for measuring solute breakthrough curves (BTC's) in the 20-cm-long, saturated soil columns; results for the 1-m-long columns will be discussed elsewhere. We show that the mass or concentration of solutes within the TDR sampling volume can be estimated effectively by measuring the bulk soil electrical conductivity using TDR. We further investigate whether existing transport models, such as the convection–dispersion equation (CDE) or mobile–immobile water (MIM) -type solute transport models, can be used to represent the observed BTC's.

Table 1
Selected physico-chemical properties of the studied soil

Particle size distribution (%)					C^a (%)	pH_{KCl}	pH_{H_2O}	CEC^b
clay	silt		sand					
0–2 μm	2–10 μm	10–20 μm	20–50 μm	50–2000 μm				
12.65	4.23	8.87	34.52	39.73	0.6	5.7	6.5	5.24

[a]Organic carbon content.
[b]meq/100 g soil.

2. Material and methods

2.1. Transport experiments

Thirty undisturbed soil columns were collected from a 35-m-long transect in a sandy loam soil (Udifluvent/Eutric Regosol) covered by grass. Selected physico-chemical properties for the A_p horizon (0–25 cm) are listed in Table 1. After clearing the soil surface of vegetation, the soil columns were isolated by excavating the soil around them. Next, 20-cm-long, 20-cm-I.D. polyvinylchloride (PVC) cylinders were placed over the isolated soil columns. The columns were subsequently cut off at the bottom using a sharpened spade. A wooden plate was attached to the bottom of the cylinders to prevent soil from falling out. The top of the columns was covered with plastic to prevent evaporation.

Once brought into the laboratory, the columns were put on a perforated PVC plate and saturated from the bottom. Parallel two-rod TDR probes, similar to those discussed by Ledieu et al. (1986), were inserted horizontally in the middle of each cylinder. The rods had a length of 15 cm and a diameter of 0.5 cm. The rods on each probe were separated by 2 cm. A 18.5-cm-diameter piece of filter paper was put on top of the column to prevent the loss of fine soil particles from the columns' top surface during leaching. Prior to application of a tracer, solute-free water was added to the soil columns by means of a Mariotte system which maintained a constant water level of $\sim$ 2 cm on top of the soil column. After reaching steady-state water flow, the input of water was interrupted and the remaining ponded water allowed to infiltrate. 50 ml of a 0.8 *M* KCl solution was subsequently applied manually to each column by uniformly spreading the solution over the soil surface. The tracer application corresponded to an instantaneous solute pulse of $\sim$ 45 g m^{-2} Cl^-, which is similar to the pulse applied by Kachanoski et al. (1992). As soon as all of the applied solute had infiltrated, distilled water was again added to the soil surface using the Mariotte system. Solute BTC's were monitored using horizontally installed TDR probes as explained in the next section. Soil water contents in the columns during the experiments were estimated using the same probes after appropriate calibration.

2.2. Estimating electrical conductivity and solute concentrations

In addition to becoming a relatively popular tool for measuring volumetric water contents in soils (e.g., Topp et al., 1982; Heimovaara and Bouten, 1990), TDR is now also increasingly being used for measuring the bulk soil electrical conductivity by making use of the attenuation of an electromagnetic wave that travels along a transmission line (Dalton and van Genuchten, 1986; Topp et al., 1988). Monitoring of in situ solute BTC's using TDR was first reported by Elrick et al. (1992) and Kachanoski et al. (1992) using vertically installed TDR probes. As opposed to these studies, results in this paper were obtained with horizontally installed TDR probes.

Application of TDR to measurements of the bulk soil electrical conductivity, EC_a, is based on the usual assumption that at a given water content, θ, a linear relationship exists between EC_a and the solution concentration, C (Kachanoski et al., 1992), i.e.:

$$C = a + bEC_a \tag{1}$$

where a and b are empirical constants. We note that, in turn, the bulk soil electrical conductivity, EC_a, can be related linearly to the electrical conductivity of the soil solution, EC_w, and the apparent solid phase electrical conductivity, EC_s, for homogeneous soil systems (e.g., Rhoades et al., 1976) as well as for structured systems containing mobile and immobile water phases (Rhoades et al., 1989).

Consider the above column displacement experiments where a tracer solution of concentration C_0 is added to a soil column having an initial concentration C_i (the latter being zero for an initially solute-free system). The concentration $C(x, t)$ and bulk electrical conductivity, $EC_a(x, t)$ become then functions of time t after application of the solute tracer pulse. The relative concentration, $c(x, t)$, at any location, x, in a soil column at time t is given by:

$$c(x, t) = [C(x, t) - C_i]/(C_0 - C_i) \tag{2}$$

or with Eq. 1:

$$c(x, t) = [EC_a(x, t) - EC_{a,i}]/(EC_{a,0} - EC_{a,i}) \tag{3}$$

which shows that the constants a and b of Eq. 1 have been eliminated. The bulk soil electrical conductivities $EC_{a,i}$ and $EC_{a,0}$ in Eq. 3 are associated with the initial and input solute concentrations, C_i and C_0, respectively, whereas $EC_{a,i}$ represents the background electrical conductivity.

An attractive way for determining the bulk soil electrical conductivity is by using TDR. Dalton and van Genuchten (1986) inferred EC_a from the attenuation of a reflected step voltage pulse guided through parallel transmission lines inserted in the soil. The voltage pulse behaves like an electromagnetic wave which loses part of its energy as it travels through the soil. The impedance or total resistance, Z, to flow of the electrical current in the soil can be obtained from a TDR cable tester. Thus, the estimate of the bulk electrical conductivity, EC_a, is obtained from the impedance load, Z (Ω), of a two-, three-, or four-rod parallel TDR probe.

Values of the impedance load, Z, are read directly from the screen of a TDR

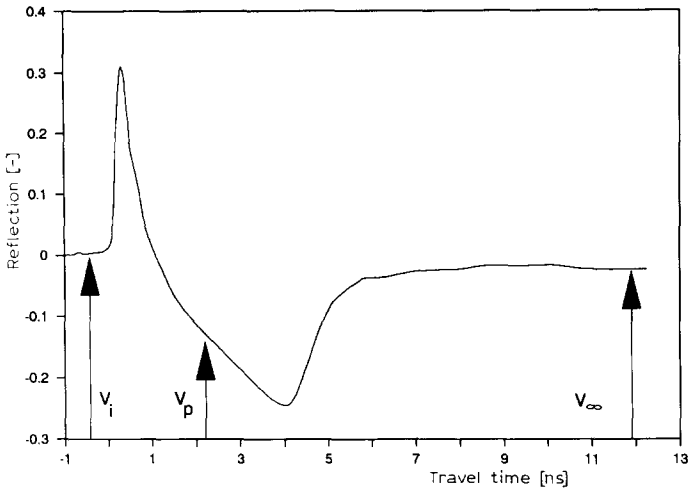

Fig. 1. TDR wave obtained from the Tektronix® cable tester using a two-rod parallel probe. V_i = input signal of the TDR pulse; V_p = signal after partial reflection from start of the probe; V_∞ = signal reflection after a long time, $t \rightarrow \infty$ (location of screen cursor for breaktrough experiment).

measuring device, e.g., a *1502*B TDR Tektronix® cable tester (Tektronix, Inc., Beaverton, Oregon, U.S.A.) connected to the parallel rods by a 50-Ω coaxial cable. Readings are made at the location where the screen cursor intersects the TDR trace. The reading is made at $t \rightarrow \infty$, when the magnitude of the final reflected signal becomes constant (Fig. 1). According to Nadler et al. (1991), the problem of multi-reflection interferences caused by impedance discontinuities can be overcome by obtaining readings of the impedance load at a very long distance along the TDR trace. All reflections are then suppressed and Z will reach a constant value. In our study, all readings of Z were obtained at a distance of 30 ft (9.144 m) (the TDR instrument displays distances along the trace instead of travel time).

Following equation (9) from Nadler et al. (1991), the bulk electrical conductivity EC_a can be obtained from:

$$EC_a = K_c f_t Z^{-1} \tag{4}$$

where K_c is a geometry constant; and f_t a temperature-correction coefficient. Inserting Eq. 4 into Eq. 3 yields for the relative concentration:

$$c(x,t) = [Z^{-1}(x,t) - Z_i^{-1}]/(Z_0^{-1} - Z_i^{-1}) \tag{5}$$

where Z_i and Z_0 are the impedance load readings associated with $EC_{a,i}$ and $EC_{a,0}$, respectively. The parameter Z_i is readily measured before application of the tracer solution. However, estimation of Z_0 is relatively more difficult, and also quite different for horizontally installed TDR probes as compared to vertically installed probes. Consider first the case of a horizontally installed probe. When a solute pulse reaches the probe at given depth x, the pulse is already dispersed and the concentration, C, within the sampling volume as seen by TDR will be less than the

input concentration, C_0. Hence, the value of Z is initially larger than Z_0 associated with concentration C_0, since $C < C_0$. Thus, Z_0 cannot be immediately obtained from the TDR reading and an alternative method must be used to estimate the equilibrium impedance associated with C_0. Alternative approaches are numerical integration of the observed Z vs. time curve (Vanclooster et al., 1993), or adding enough tracer solution such that the solution concentration at depth x reaches the input concentration, C_0 (this study). Both of these approaches have their advantages and disadvantages. While relatively quick and easy to implement, a disadvantage of the first approach is that it requires complete mass recovery. The second approach on the other hand, may require the application of a long solute pulse to ensure that the solute concentration will reach the same value everywhere in the sampled volume.

The above analysis for horizontal probes is different for vertically installed TDR probes. Assuming that the vertical TDR probe extends from the surface to a depth L, addition of a solute pulse with total mass M at time t_0 will immediately lead to a quick drop in the impedance load Z. As long as the finite solute pulse is located entirely within the sampling volume of the TDR, the impedance load will have a constant and minimum value Z_0 associated with the total solute mass M. However, as the solute pulse moves below the bottom end of the TDR probe, the impedance will gradually increase and eventually reach its original value Z_i when all the solute has moved below the probe. The difference between Z_i and Z_0 is subsequently used in the calibration process to obtain relative mass distributions (Kachanoski et al., 1992), from which, in turn, flux concentrations at $x = L$ can be derived (Elrick et al., 1992).

3. BTC data analysis

Once constructed from the measured TDR impedance loads, all BTC's were analyzed in terms of time moments. The nth normalized temporal moment, μ_n', at depth x for a pulse input is (e.g., Leij and Dane, 1991):

$$\mu_n' = m_n/m_0 = \int_0^\infty t c(x,t)\mathrm{d}t \Big/ \int_0^\infty c(x,t)\mathrm{d}t \tag{6}$$

where m_n is the nth temporal moment; and m_0 the zeroth moment. The value of m_0 corresponds to the total mass added to the soil, i.e. $m_0 = C_0 t_0$. If reduced concentrations are used, i.e. $C_0 = 1$, the zeroth moment gives immediately the pulse time t_0. The first normalized moment can be used to characterize the mean displacement time, i.e. $\mu_1' = m_1/m_0$. Using the mean estimated breakthrough time, μ_1', we define an effective velocity, v_{eff}, as:

$$v_{\mathrm{eff}} = x \Big/ \left(\mu_1' - \frac{1}{2}t_0\right) \tag{7}$$

The variance, or second central moment, μ_2, defines the spread relative to the mean

breakthrough time:

$$\mu_2 = m_0^{-1} \int_0^{\infty} (t - \mu_1')^2 c(x,t) \mathrm{d}t \tag{8}$$

Although higher-order moments in Eq. 6 are easily evaluated, their values are generally not very reliable or useful because of the disproportionate effect of data in the tail end of the BTC at relatively large times. These data are usually also most vulnerable to calibration errors, including those resulting from a poorly defined Z_0. We also define the coefficient of skewness $SK = \mu_3/\mu_2^{3/2}$, whose value indicates whether the shape of a BTC is symmetrical, or positively or negatively skewed.

The observed BTC's were also analyzed in terms of two popular solute transport models, i.e. the CDE, and a MIM-type nonequilibrium model which accounts for the presence of distinct mobile and immobile liquid phases in the soil.

The transport of linearly adsorbing solutes in a one-dimensional flow system is described by the CDE:

$$\frac{\partial C}{\partial t} = D\frac{\partial^2 C}{\partial x^2} - v\frac{\partial C}{\partial x} \tag{9}$$

where C is the volume-averaged or resident concentration (g cm^{-3}); D the dispersion coefficient (cm^2 h^{-1}); $v = q/\theta$, the average pore-water velocity (cm h^{-1}); q the Darcian water flux (cm h^{-1}); θ the volumetric water content (cm^3 cm^{-3}); x is distance in cm (positive downward); and t is time (h).

To account for the often observed asymmetry or tailing of column effluent curves, van Genuchten and Wierenga (1976), among others, formulated a MIM water model which assumes that the soil liquid phase consists of mobile (dynamic) and immobile (stagnant) soil-water regions. Convective–dispersive transport is assumed to occur only in the mobile phase while exchange of solutes between both liquid phases is diffusion controlled and modelled by means of a first-order rate expression. Assuming steady-state water flow, the transport equations for the MIM model are:

$$\theta_m \frac{\partial C_m}{\partial t} + \theta_{im} \frac{\partial C_{im}}{\partial t} = \theta_m D_m \frac{\partial^2 C_m}{\partial x^2} - q\frac{\partial C_m}{\partial x} \tag{10}$$

$$\theta_m \frac{\partial C_{im}}{\partial t} = \alpha(C_m - C_{im}) \tag{11}$$

where θ_m is the mobile water content and θ_{im} the immobile water content such that $\theta = \theta_m + \theta_{im}$; C_m the solute concentration in the mobile region; C_{im} is the concentration of the immobile region; $v_m = q/\theta_m$ is the average pore-water velocity in the mobile liquid phase; D_m is the dispersion coefficient in the mobile phase; and α is a mass-transfer coefficient determining the rate of exchange between the two liquid phases (h^{-1}). For the MIM model, the total resident concentration, C_T, is given by:

$$C_T = (\theta_m/\theta)C_m + (1 - \theta_m/\theta)C_{im} \tag{12}$$

Analytical solutions for a third-type inlet condition and a semi-infinite system were used for fitting the transport parameters in the above CDE and MIM models using the CXTFIT nonlinear parameter estimation code of Parker and van Genuchten

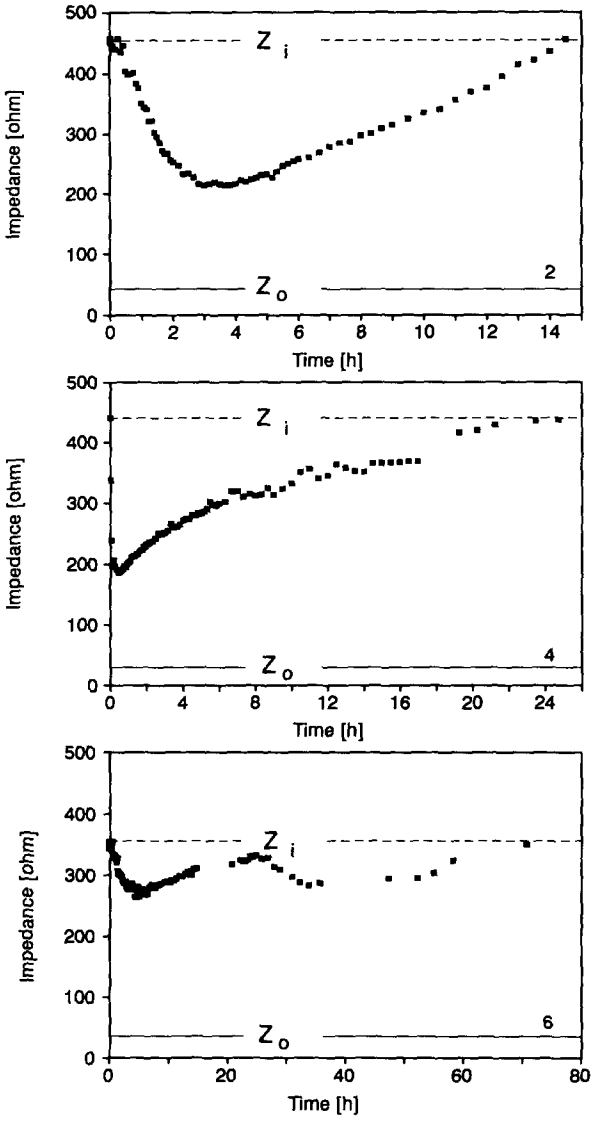

Fig. 2. Impedance load $Z(x, t)$ for a pulse-type injection of KCl using horizontally inserted TDR probes.

(1984). We note again that TDR probes presumably measure total resident concentrations; hence the CXTFIT code required some revisions to enable the use of total resident concentration in the parameter optimization approach.

4. Results

Measured values for the impedance, Z, for three typical solute BTC's are shown in

Table 2
Experimental time moments of the observed nonreactive solute breakthrough curves

No.	m_0 (h)	μ_1' (h)	μ_2 (h^2)	SK (–)	v_{eff} (cm h^{-1})	v_0 (cm h^{-1})
1	0.81	6.8	30.1	1.77	1.57	38.0
2	0.70	5.5	9.1	0.43	1.93	8.82
3	2.55	14.8	114.6	0.82	0.74	15.9
4	0.51	6.4	28.9	0.84	1.62	15.5
5	0.46	5.9	16.0	72.6	1.76	8.00
6	0.91	30.4	325.7	−0.08	0.33	1.44

m_0 = zeroth moment; μ_1' = mean breakthrough time; μ_2 = variance; SK = coefficient of skewness.

Fig. 2. The initial load, Z_i, before application of the solute pulse varied considerably among the different columns, ranging from $\sim$ 100 to $\sim$ 600 Ω. This variation may be due to local changes in EC_a near the soil surface, probably as a result of heterogeneities in clay content, or previous nonuniform applications of Ca-rich amendments to the field site.

The measured values for Z_i and Z_0 were used to normalize the observed impedance curves into relative concentrations between 0 and 1. Figs. 3–5 present three types of BTC's thus obtained. Fig. 3 shows type-1 BTC's which, typically, are bell-shaped or only slightly skewed, and appear to reflect transport consistent with the CDE model. Type-2 BTC's, shown in Fig. 4, exhibited fast breakthrough and extensive asymmetry and/or tailing. Asymmetric solute transport behaviour is known to occur in many structured soils containing relatively permeable (macropore) regions which facilitate the relative fast downward movement of water and dissolved solutes. Simultaneously, solute will move laterally by diffusion into and out of stagnant soil water phases, thus creating early breakthrough and tailing as shown by the curves in Fig. 4. Finally, type-3 BTC's shown in Fig. 5 exhibit multiple peaks, suggesting the presence of a bimodal (or even a multi-modal) porous medium. In this case, dissolved solutes may be transported relatively quickly through one or more preferential flow paths, and more slowly through the bulk soil matrix, with limited interactions between the different flow regions. Although the above three types of BTC's do not necessarily represent solute behaviour at the scale of an entire column, they do show that, at least at the scale of sampling, a variety of solute transport processes occur.

Results of the moment analysis for 6 typical columns are presented in Table 2. Notice that the zeroth-order moment, m_0, and the mean breakthrough time, μ_1', varied considerably among the columns. Even more variable was the variance (μ_2) or the spreading of the solute pulse around the mean breakthrough time. The shape of the BTC's were quantified by means of the skewness coefficient (SK). Both symmetrical (SK $\approx$ 0) and highly positively skewed BTC's are represented in Table 2. Symmetrical BTC's are consistent with Fickian-type convection–dispersion transport, whereas asymmetrical curves suggest the presence of some type of non-equilibrium transport process. Table 2 also compares the effective velocity, v_{eff}, as calculated with Eq. 7 with the measured velocity, $v_0 = q/\theta$. Notice that the actual

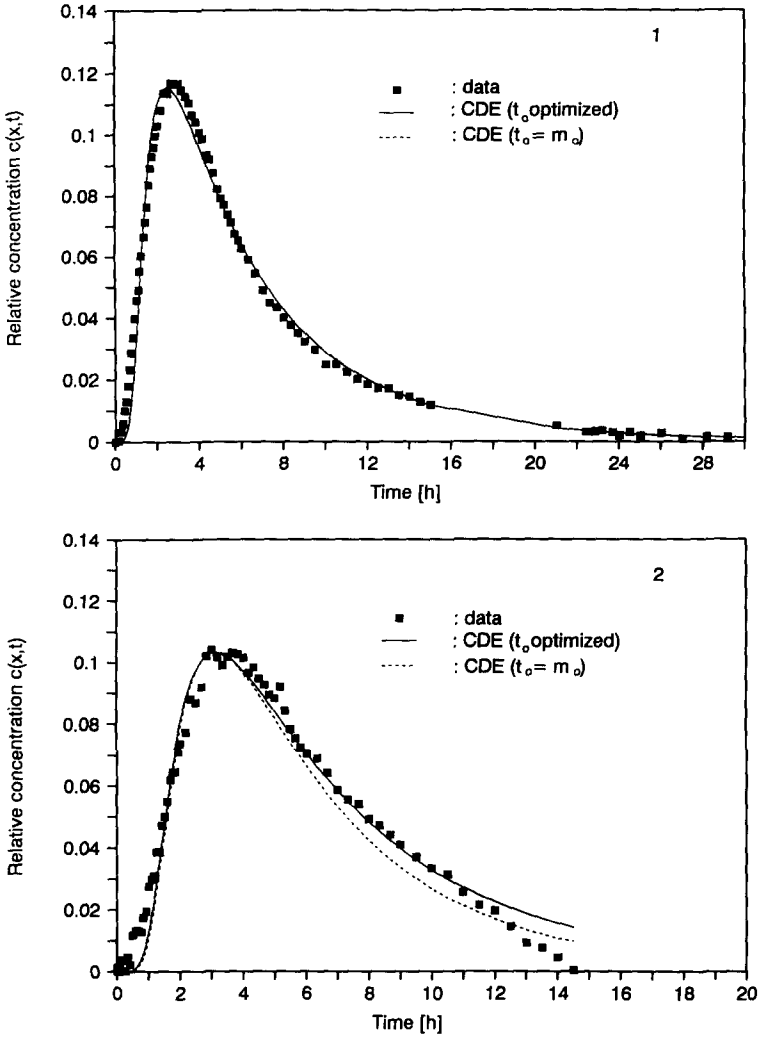

Fig. 3. Typical type-1 BTC measured with TDR probes at 10-cm depth in an undisturbed saturated soil column.

average pore-water velocity (v_0) is always much larger than the effective velocity obtained directly from the measured BTC's. This result suggests that TDR measures equally the slower transport regions in the column. From Table 2 it is evident that the transport data exhibit much variability and that the two process-based transport models can be applied to only particular subsets of the data.

Because of the disparity between v_{eff} and v_0, the parameter optimization code CXTFIT was first used to fit the parameters t_0, v and D (case *1*) to the observed BTC's. The fitted values for the pore-water velocity (denoted here by v_s) and the dispersion coefficient, D, for the CDE model are listed in Table 3 for selected

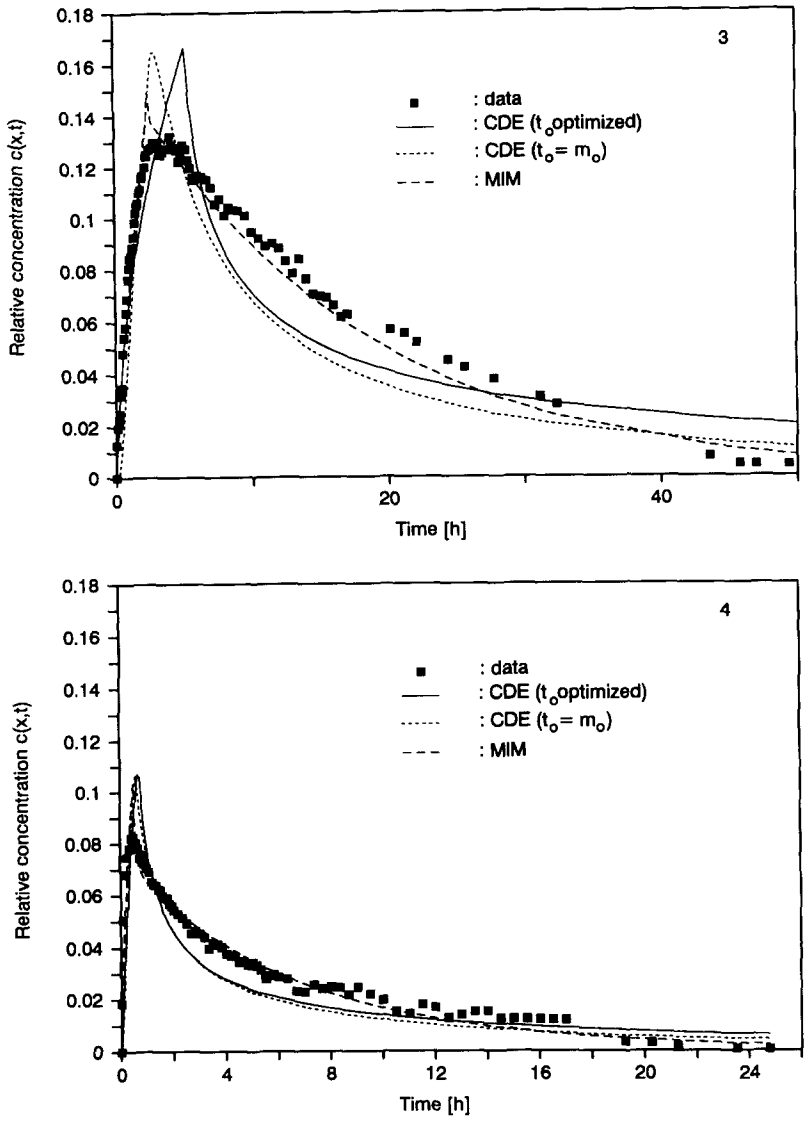

Fig. 4. Typical type-2 BTC measured with TDR probes at 10-cm depth in an undisturbed saturated soil column.

BTC's. As can be seen from Fig. 3, type-1 BTC's are well fitted by the CDE model, resulting for example in a dispersion coefficient of 12.84 and 8.57 $cm^2\ h^{-1}$ for columns *1* and *2*, respectively. However, the CDE model is not able to produce a good fit for the type-2 BTC's, such as those for columns *3* and *4* shown in Fig. 4. This also follows from the data in Table 3, which shows that the coefficient of determination r^2 of type-2 BTC's is $\sim 10\%$ less as compared to the type-1 data. Moreover, as expected, optimized *D*-values for the type-2 curves are much larger, and have higher standard

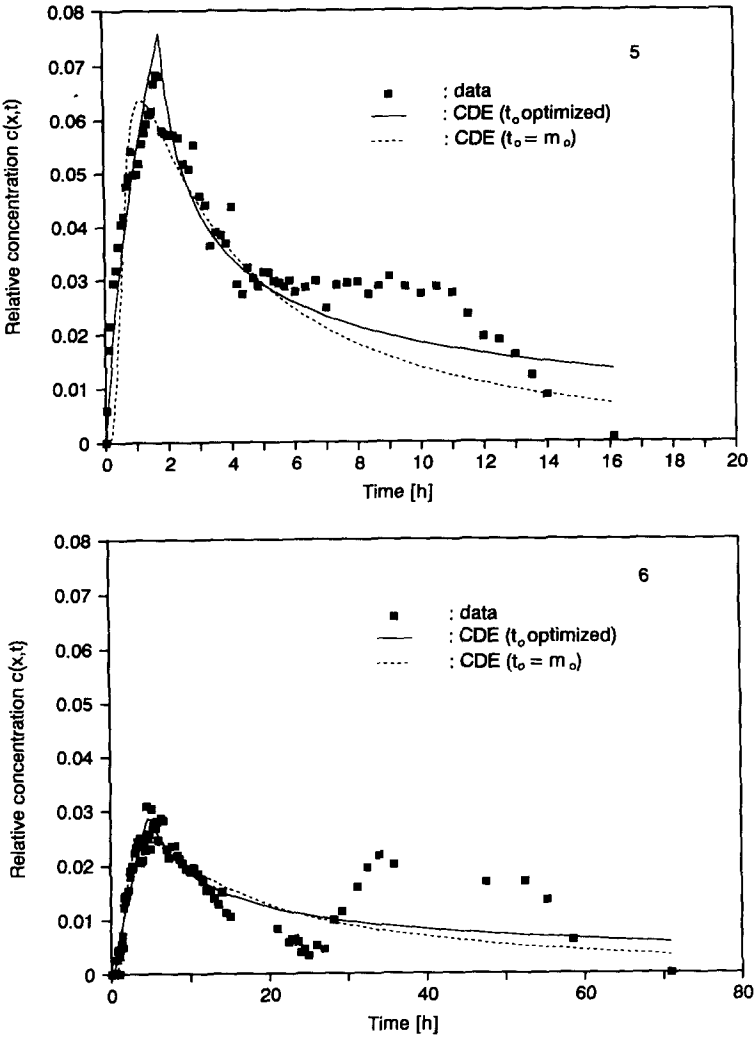

Fig. 5. Typical type-3 BTC measured with TDR probes at 10-cm depth in an undisturbed saturated soil column.

errors, as those for Type-1 curves. Although it is evident from Fig. 5 that multi-peak BTC's cannot be fitted with the simple CDE model, results are given here only to provide a visual comparison with the previous simulations.

We also fitted the nonequilibrium MIM model (Eqs. 10 and 11) to type-2 BTC's (Fig. 4). Fitted parameters for the two curves in Fig. 4 are listed in Table 4. Notice the very small values of the fraction mobile water, θ_m/θ, indicating that only a small fraction of the pore space contributes to the convective transport process. The potentially very significant effects of immobile water, and the associated diffusion of solutes into and out of the immobile water phase, is further illustrated in Figs. 6

Table 3
Solute transport parameters obtained by fitting the CDE model to the experimental BTC for case *1* (t_0 is optimized) and for case *2* ($t_0 = m_0$)

Column	v_0 (cm h^{-1})	θ (cm^3 cm^{-3})	t_0 (h)	v_s (cm h^{-1})	D (cm^2 h^{-1})	r^2
Three-parameter fit (t_0, v_s, D):						
1	1.58	0.42	0.808 (0.02)	2.338 (0.04)	12.84 (0.48)	0.984
2	11.87	0.37	0.799 (0.02)	2.001 (0.05)	8.57 (0.39)	0.971
3	21.95	0.39	5.235 (0.09)	3.123 (0.07)	1660.00 (82)	0.851
4	8.99	0.38	0.694 (0.06)	5.224 (0.73)	868.30 (425)	0.859
5	3.29	0.37	1.753 (0.07)	1.939 (0.29)	860.70 (361)	0.909
6	2.00	0.36	4.398 (0.45)	0.160 (0.02)	50.15 (6.83)	0.815
Two-parameter fit (v_s, D):						
1	1.58	0.42	0.809[a]	2.336 (0.02)	12.87 (0.30)	0.984
2	11.87	0.37	0.704[a]	2.159 (0.27)	7.41 (0.25)	0.973
3	21.95	0.39	2.550[a]	1.458 (0.05)	49.37 (5.65)	0.874
4	8.99	0.38	0.508[a]	5.010 (0.35)	34.90 (0.22)	0.763
5	3.29	0.37	0.457[a]	2.635 (0.09)	42.01 (3.89)	0.850
6	2.00	0.36	0.912[a]	0.516 (0.01)	9.99 (0.66)	0.798

For both cases, $R = 1$ is fixed. Standard error is given between parentheses.
[a] t_0 estimated from zeroth moment (Table 2).

and 7. Fig. 6 shows calculated equilibrium (mobile water phase *1*) and nonequilibrium (immobile water phase *2*) resident concentrations obtained with MIM parameters of column *4*, while Fig. 7 gives for this same column the relative amounts of mass of solute in the mobile phase, i.e. $(\theta_m/\theta)C_m$, and that in the immobile water phase, i.e. $(1 - \theta_m/\theta)C_{im}$. Because of the very small value of θ_m/θ, generally only a small fraction of the solute resides in the mobile phase, even though the peak concentration in the mobile phase is much higher than that in the immobile phase.

Table 4
Solute transport parameters obtained by fitting the MIM model to the experimental BTCs of columns *3* and *4*

Column	t_0 (h)	v_s^a (cm h^{-1})	D^b (cm^2 h^{-1})	θ_m/θ (–)	α (h^{-1})	r^2
3	2.550[c]	2.58 (0.35)	3.09 (9.75)	0.026 (0.008)	0.03 (0.007)	0.971
4	0.508[c]	2.76 (0.07)	25.0 (3.66)	0.020 (0.005)	0.66 (0.040)	0.939

Standard error is given between parentheses.
[a] $v_s = v_m(\theta_m/\theta)$.
[b] $D = D_m(\theta_m/\theta)$.
[c] t_0 estimated from zeroth moment.

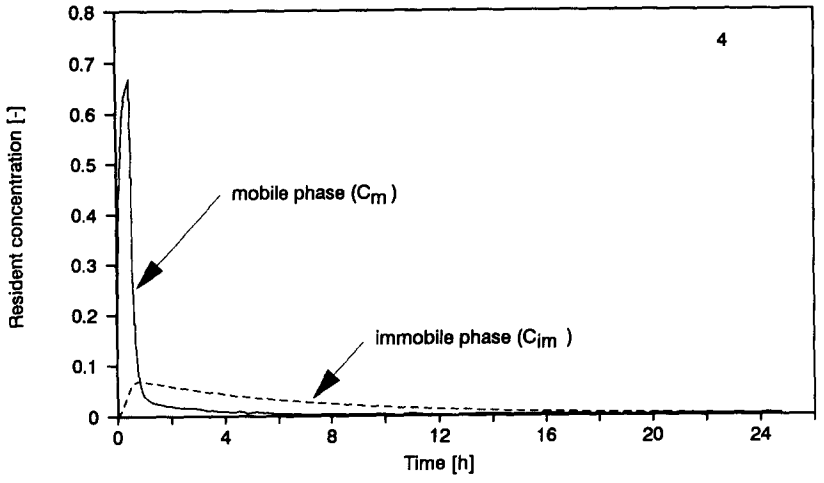

Fig. 6. Predicted resident concentration profiles for phase-*1* (mobile) and phase-*2* (immobile) regions in soil column *4*.

5. Discussion

The experiments discussed above show that TDR is a simple and relatively cheap method for obtaining solute BTC's in laboratory experiments. Moreover, the BTC can be obtained in an almost undisturbed fashion. Although the BTC's in this study were monitored at only one depth, several TDR probes could be easily inserted at different depths in a soil column with only minimal disturbances of the flow-path. This feature allows accurate monitoring of solute transport, for example in the vicinity of interfaces between soil layers. Also, by averaging of the BTC's obtained

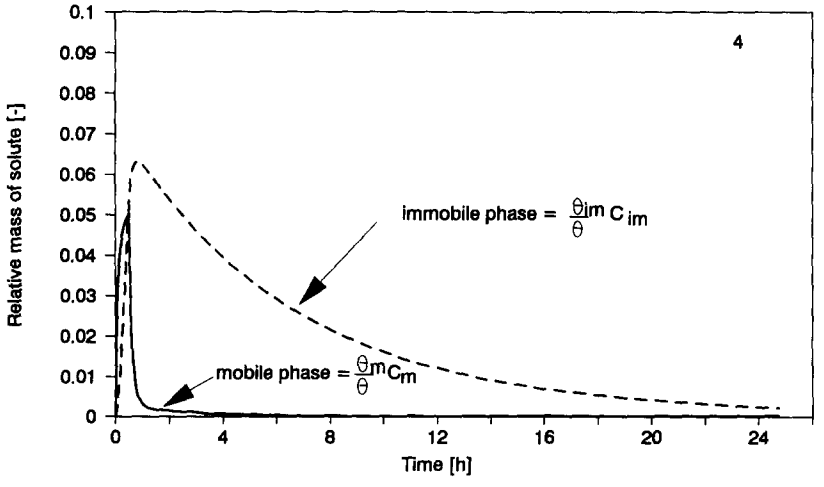

Fig. 7. Predicted total solute mass profiles for phase-*1* (mobile) and phase-*2* (immobile) regions in soil column *4*.

through several probes inserted at the same depth, more representative BTC's for the entire column cross-section can be derived.

As compared to BTC's obtained from effluent data, one of the disadvantages of the TDR technique is the smaller area or volume of soil that is sampled. For a rod diameter of 0.5 cm, a distance between the rods of 2 cm, and rod lengths of 15 cm, one may calculate that the effective sampling volume of the TDR covers ~ 90 cm^2 or $\sim 30\%$ of the cross-sectional area of the soil columns. This calculation assumes that 95% of the TDR wave energy is contained within the sampling area [see equation (49) of Knight (1992)]. Measuring over only 30% of the cross-section increases the chance of not detecting the entire solute plume, especially when preferential flow paths are present. By comparison, vertically installed TDR probes, would have reduced the influence region to ~ 28 cm^2, or only $\sim 9\%$ of the total cross-sectional area. Still, as compared to uncertainties associated with the very small effective sampling areas as seen by porous cups, we believe that TDR offers a viable technique for in situ solute BTC monitoring. Moreover, when the flow field inside columns is very heterogeneous due to soil structure, such as was the case in our columns, several TDR probes could be installed orthogonal to each other to increase the effective sampling volume.

Curve-fitting of the CDE model to three types of BTC's obtained in this study in general showed good agreement with the observed data and resulted in reasonable values of the dispersion coefficient. However, this could only be obtained by estimating t_0 from the zeroth time moment. Estimating t_0 from the zero-order moment produced less uncertainty in v_s and D (since fewer parameters were fitted) and resulted in an apparent conservation of the solute mass. The use of experimental time moments is justified because they provide a physically meaningful technique for characterizing BTC's independent of the invoked transport model.

In this study we compared CDE and MIM solute transport models at one single depth along the flow path. From a fitting point of view, the MIM model should always give better results as compared to the CDE because of the higher number of parameters. Also, Khan and Jury (1990) and Jury et al. (1991) pointed out that testing of a model assumption can only be done by monitoring solute behaviour at several different distances from the inlet point. This is especially true when studying possible scale-dependent phenomena (e.g., an increase in the dispersion coefficient, D, with transport distance). Therefore, observations of solute movement at different depths in large undisturbed soil columns will be a major concern in our future experiments.

A comparison of the simulated (cases *1* and *2*, Table 3) vs. measured pore velocities revealed that the former may have been underestimated, or the latter overestimated. For this reason we used the effective velocity (v_{eff}) calculated with Eq. 7 to decide which velocity was most appropriate for the BTC's measured in the sampling volume of the TDR probes. The values of v_{eff} (Table 2) suggest that the estimated (optimized) v_s is more appropriate. This seems surprising since measurements of the drainage flux from a soil column are relatively easy to make. We believe that, contrary to the analysis of BTC's using effluent data, TDR only samples a small region of the whole flow domain. This region may or may not include preferential flow channels. The existence of macropores was evaluated by adding methylene blue dye to the soil

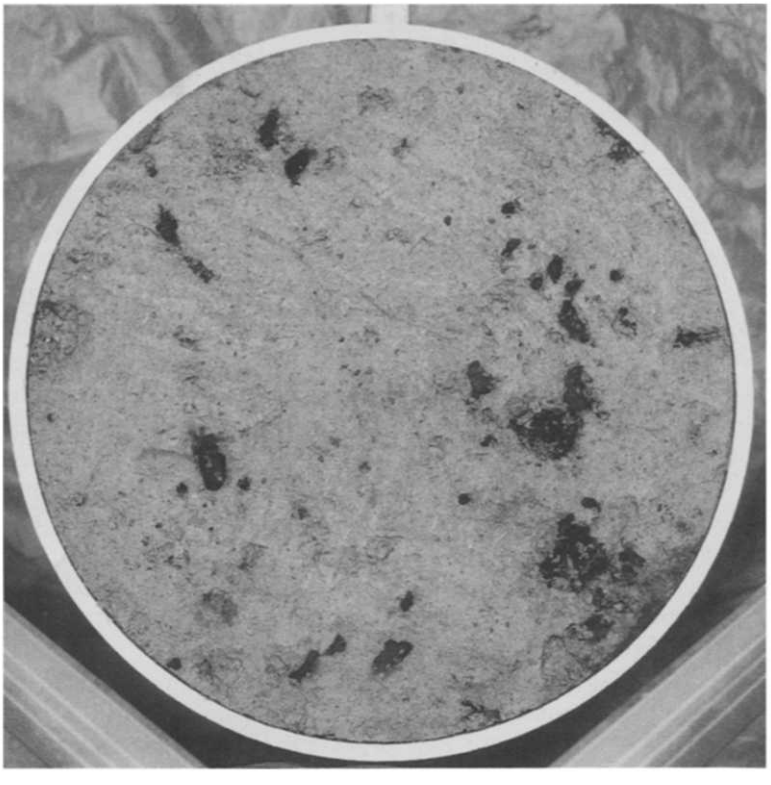

Fig. 8. Stained dye pattern indicating the presence of macropores.

surface under ponding conditions. A picture of the stained dye pattern taken just below the TDR probe is shown in Fig. 8. Clearly identifiable macropores were present in all columns. If the sampling volume does not contain a macropore, only the slow matrix transport part will be detected, thus ignoring the high-velocity flow areas, and leading to lower fitted pore-water velocities. Therefore, when preferential flow in structured soils is expected, one may want to increase the sampling volume of the soil by additional TDR probes orthogonal to the first. Another alternative would be to increase the sampling volume of the probes by increasing the distance between the probe wires, or by reducing the wire diameter. This could be done for two-rod probes as well as for coaxial-emulating three-wire and multi-wire probes, as long as the ratio of half the wire spacing to the wire diameter remains less than ~ 10 (Knight, 1992).

6. Conclusions

Solute BTC's in saturated soil columns were monitored using horizontally inserted TDR probes. Interpretation of the signal impedance was done in a way similar to Kachanoski et al. (1992), but now involving a continuous application of the tracer

solution in order to obtain estimates of the minimum impedance load, Z_0. Applying time moments to the data revealed considerable variability among the parameters. When the effective velocity (v_{eff}) was calculated based on the mean breakthrough time of the BTC, large disparities between the measured velocities (v_0) existed. Better agreement was found between v_{eff} and the fitted v_s for the CDE model. From these analyses we conclude that the flow field inside the column was essentially three-dimensional and heterogeneous. When the CDE and MIM solute transport models were fitted to a subset of the observed data, both models yielded results that were satisfactory, provided the average pore-water velocity v_s and the dispersion coefficient D were optimized, and the application time t_0 was put equal to the zeroth time moment. Analysis of the BTC's in terms of the MIM water model revealed a small percentage of mobile water and a transport process dominated by solute diffusion between immobile and mobile regions.

Since its application is simple, cheap (no chemical analysis cost) and only minimally disturbs the flow pattern of the tracer, it is to be expected that the TDR technique will become a widely used method for measuring BTC's, both in the laboratory as well as under field conditions, provided accurate calibration procedures can be established. Structured soils may require a larger number of probes in order to obtain estimates of the solute transport process at scales several times larger than the scale of observation. This result is evident from our analysis involving laboratory soil columns, but may be even more pertinent for field measurements. Another advantage of the TDR method is that soil water contents can be determined on the same sampling volume. Automization of the system could make TDR very suitable for collecting long time series, both in the laboratory and even more so in remote field areas. Finally, we believe that TDR should not be used to replace existing monitoring techniques such as soil coring or vacuum application with porous cups, but rather as an additional tool for providing information on subsurface solute transport behaviour.

Acknowledgements

The authors are grateful to M.Th. van Genuchten and N. Toride from the U.S. Salinity Laboratory, Riverside, California, for using the modified CXTFIT code, and for their helpful comments and suggestions. The authors would also like to thank the anonymous referees for their comments which improved the readability of the paper.

References

Alberts, E.E., Burnell, R.E. and Schuman, G.E., 1977. Soil nitrate-nitrogen determined by coring and solution extraction techniques. Soil Sci. Soc. Am. J., 41: 90–92.

Biggar, J.W. and Nielsen, D.R., 1962. Miscible displacement, 2. Behavior of tracers. Soil Sci. Soc. Am. Proc., 26: 125–128.

Broadbent, F.E., 1981. Methodology for nitrogen transformation and balance in soil. Plant Soil, 58: 383–399.

Butters, G.L., Jury, W.A. and Ernst, F.F., 1989. Field scale transport of bromide in an unsaturated soil, 1. Experimental methodology and results. Water Resour. Res., 25: 1575–1581.

Dalton, F.N. and van Genuchten, M.Th., 1986. The time-domain reflectometry method for measuring soil water content and salinity. Geoderma, 38: 237–250.

Ellsworth, T.R., Jury, W.A., Ernst S.S. and Shouse, P.J., 1991. Three-dimensional field study of solute transport through unsaturated layered porous media, 1. Methodology, mass recovery, and mean transport. Water Resour. Res., 27: 951–965.

Elrick, D.E., Kachanoski, R.G., Pringle, E.A. and Ward, A., 1992. Parameter estimation of field solute transport models based on time domain reflectometry measurements. Soil Sci. Soc. Am. J., 56: 1663–1666.

Hansen, E.A. and Harris, A.R., 1975. Validity of soil-water samples with porous ceramic cups. Soil Sci. Soc. Am. Proc., 39: 528–536.

Heimovaara, T.J. and Bouten, W., 1990. A computer-controlled 36-channel time-domain reflectometry system for monitoring soil water contents. Water Resour. Res., 26: 2311–2316.

Jury, W.A., Stolzy, L.H. and Shouse, P., 1982. A field test of the transfer function model for predicting solute transport. Water Resour. Res., 18: 369–375.

Jury, W.A., Gardner, W.R. and Gardner, W.H., 1991. Soil Physics. Wiley, New York, NY, 5th ed., 328 pp.

Kachanoski, R.G., Pringle, E.A. and Ward, A., 1992. Field measurement of solute travel times using time domain reflectometry. Soil Sci. Soc. Am. J., 56: 47–52.

Khan, A.U.-H, and Jury, W.A., 1990. A laboratory study of the dispersion scale effect in column outflow experiments. J. Contam. Hydrol., 5: 119–131.

Knight, J.H., 1992. Sensitivity of time domain reflectometry measurements to lateral variation in soil water content. Water Resour. Res., 28: 2345–2352.

Ledieu, J., De Ridder, P., De Clerck, P. and Dautrebande, S., 1986. A method of measuring soil moisture by time-domain reflectometry. J. Hydrol., 88: 319–328.

Leij, F.J. and Dane, J.H., 1991. Solute transport in a two-layer medium investigated with time moments. Soil Sci. Soc. Am. J., 55: 1529–1535.

Nadler, A., Dasberg, S. and Lapid, I., 1991. Time domain reflectometry measurements of water content and electrical conductivity of layered soil columns. Soil Sci. Soc. Am. J., 55: 938–943.

Parker, J.C. and van Genuchten, M.Th., 1984. Determining transport parameters from laboratory and field tracer experiments. Va. Agric. Exp. Stn., Blacksburg, VA, Bull. 84-3.

Rhoades, J.D., Raats, P.A.C. and Prather, R.J., 1976. Effects of liquid-phase electrical conductivity, water content, and surface conductivity on bulk electrical conductivity. Soil Sci. Soc. Am. J., 40: 651–655.

Rhoades, J.D., Manteghi, N.A., Shouse, P.J. and Alves, W.J., 1989. Soil electrical conductivity and soil salinity: new formulations and calibrations. Soil Sci. Soc. Am. J., 53: 433–439.

Schulin, R., Wierenga, P.J., Flühler, H. and Leuenberger, J., 1987. Solute transport through a stony soil. Soil Sci. Soc. Am. J., 51: 36–42.

Seyfried, M.S. and Rao, P.S.C., 1987. Solute transport in undisturbed columns of an aggregated tropical soil: preferential flow effects. Soil Sci. Soc. Am. J., 51: 1434–1443.

Topp, G.C. and Davis, J.L., 1985. Time-domain reflectometry (TDR) and its applications to irrigation scheduling. Adv. Irrig., 3: 107–127.

Topp, G.C., Davis, J.L. and Annan, A.P., 1982. Electromagnetic determination of soil water content using TDR, I. Applications to wetting fronts and steep gradients. Soil Sci. Soc. Am. J., 46: 672–678.

Topp, G.C., Yanuka, M., Zebchuk, W.D. and Zegelin, S., 1988. Determination of electrical conductivity using time domain reflectometry: soil and water experiments in coaxial lines. Water Resour. Res., 27: 945–952.

Tyler, D.D. and Thomas, G.W., 1981. Chloride movement in undisturbed soil columns. Soil Sci. Soc. Am. J., 45: 459–461.

Vanclooster, M., Mallants, D., Diels, J. and Feyen, J., 1993. Determining local scale solute transport parameters using time domain reflectometry (TDR). J. Hydrol., 148: 93–107.

van der Ploeg, R.R. and Beese, F., 1977. Model calculations for the extraction of soil water by ceramic cups and plates. Soil Sci. Soc. Am. J., 41: 466–470.

van Genuchten, M.Th. and Wierenga, P.J., 1976. Mass transfer studies in sorbing porous media, I. Analytical solutions. Soil Sci. Soc. Am. J., 40: 473–480.

van Genuchten, M.Th. and Wierenga, P.J., 1977. Mass transfer studies in sorbing porous media, II. Experimental evaluation with tritium. Soil Sci. Soc. Am. J., 41: 272–278.

Van Wesenbeeck, I.J. and Kachanoski, R.G., 1991. Spatial scale dependence of in situ solute transport. Soil Sci. Soc. Am. J., 55: 3–7.